Chiral Confinement in Quasirelativistic Bose-Einstein Condensates

M. Merkl,[1] A. Jacob,[2] F. E. Zimmer,[1] P. Öhberg,[1] and L. Santos[2]

[1]SUPA, Department of Physics, Heriot-Watt University, Edinburgh, EH14 4AS, United Kingdom
[2]Institute for Theoretical Physics, Appelstrasse 2, Leibniz University, Hannover, Germany

(Received 25 August 2009; published 18 February 2010)

In the presence of a laser-induced spin-orbit coupling an interacting ultracold spinor Bose-Einstein condensate may acquire a quasirelativistic character described by a nonlinear Dirac-like equation. We show that as a result of the spin-orbit coupling and the nonlinearity the condensate may become self-trapped, resembling the so-called chiral confinement, previously studied in the context of the massive Thirring model. We first consider 1D geometries where the self-confined condensates present an intriguing sinusoidal dependence on the interparticle interactions. We further show that multidimensional chiral confinement is also possible under appropriate feasible laser arrangements, and discuss the properties of 2D and 3D condensates, which differ significantly from the 1D case.

DOI: 10.1103/PhysRevLett.104.073603 PACS numbers: 42.50.Gy, 03.75.−b, 37.10.De, 42.25.Bs

Although cold gases are typically neutral, artificial electromagnetism may be induced by several means, including rotation [1], manipulation of atoms in optical lattices [2–4], and the use of laser arrangements [5]. Interestingly, seminal experiments on optically created gauge fields have been recently reported [6,7]. Artificial electromagnetism has attracted growing attention in recent years, partially due to the possibility of achieving non-Abelian gauge fields [4,5], which establish fascinating links between cold gases and high-energy physics [4,8,9]. A striking example is given by the possibility of inducing quasirelativistic physics in cold atoms despite the extremely low velocities involved [10]. In particular, under proper conditions cold atoms experience an effective spin-orbit (SO) coupling, which leads to a Dirac cone in the dispersion [11], resembling the case of yet another paradigm of modern physics, namely graphene [12,13]. Similar phenomena are expected in cold atoms and graphene including Veselago lensing [10,14,15].

Interparticle interactions lead to inherent nonlinearities in Bose-Einstein condensates (BECs). At low-enough temperatures a BEC is described by a nonlinear Schrödinger equation as is the case also in nonlinear optics [1]. Resemblances between both fields have been successfully explored in recent years, most remarkably concerning solitons [16–20], for which nonlinearity and dispersion compensate each other leading to self-confinement. Nonlinearity is also important in high-energy physics, where nonlinear Dirac equations (NLDEs), and more generally nonlinear spinor fields, have been studied extensively since the pioneering works of Ivanenko [21], Weyl [22], and Heisenberg [23]. Self-confinement has attracted also in this context a large interest [24,25].

In this Letter we explore the nonlinear physics of a multicomponent BEC (also called spinor BEC [26]) in the presence of an optically induced SO coupling. In the low-momentum limit, the spinor BEC may be described by a particular type of two-component NLDE. We show that under appropriate conditions, the BEC may become self-trapped (in the absence of any external trap), resembling chiral confinement, previously discussed in the context of the massive Thirring and Gross-Neveu models [27,28]. In the present Letter, the self-confinement results from the interplay between the inherent chiral nature of the SO coupled gas and the nonlinearities which stem from the interparticle interactions. Contrary to two-component vector solitons, discussed in nonlinear optics and cold gases [29,30], the two components are coupled not only by the interactions, but also by the SO coupling as well. This opens up novel scenarios for nonlinear atom optics with condensates, characterized by remarkable new features of the self-localized BECs, which in 1D present a peculiar sinusoidal dependence of the interaction strength. Furthermore, in short-range interacting BECs solitons are stable only in 1D, whereas in 2D and 3D they are fundamentally unstable due to transversal excitations [31]. On the contrary, as discussed below, 2D and even 3D self-confinement becomes possible by means of feasible laser arrangements, where the properties of the self-trapped BECs depend strongly on dimensionality.

We consider bosons with an accessible internal tripod scheme formed by three ground $F = 1$ states ($m_F = 0, \pm 1$) and an excited $F = 0$ state [e.g., $5S_{1/2}(F = 1) \leftrightarrow 5P_{3/2}(F = 0)$ in ^{87}Rb]. The ground-state levels with $m_F = -1$, 0, and 1 are linked to the excited state by three lasers with, respectively, σ_+, π, and σ_- polarizations, Rabi frequencies $\Omega_{1,2,3}(\mathbf{r})$, and phases $S_{1,2,3}(\mathbf{r})$. The atom-light interaction leads to two dark states $|D_{1,2}(\mathbf{r})\rangle$, which are linear superpositions of the ground states. If $\Omega = (\sum_i \Omega_i^2)^{1/2}$ is large compared to any other energy (difference between the laser frequencies, Doppler and Zeeman shifts, interaction energy), we can neglect transitions out of the dark-state manifold. Assuming that the atoms are loaded into this manifold we may express any general state as $|\Psi(\mathbf{r}, t)\rangle = \sum_{i=1}^{2} \Psi_i(\mathbf{r}, t)|D_i(\mathbf{r})\rangle$, where $\Psi_i(\mathbf{r}, t)$ is the wave function for atoms in $|D_i\rangle$. By using the

Schrödinger equation for the tripod scheme, including the atomic motion, and projecting onto the dark-state manifold, one finds the effective Schrödinger equation [5]

$$i\hbar\frac{\partial}{\partial t}\vec{\Psi} = \left[\frac{1}{2m}(\mathbf{p}-\mathbf{A})^2 + \mathbf{V} + \mathbf{\Phi}\right]\vec{\Psi}, \qquad (1)$$

where $\vec{\Psi}^T = (\Psi_1, \Psi_2)$, $\mathbf{p}$ is the momentum operator, and m is the atomic mass. The spatial dependence of the laser arrangement leads to an effective vector potential matrix (also called the Mead-Berry connection [32–34]) $\mathbf{A}_{nm} = i\hbar\langle D_n(\mathbf{r})|\nabla D_m(\mathbf{r})\rangle$. In addition, $\mathbf{V}_{nm} = \sum_{j=-1}^{1} U_j\langle D_n(\mathbf{r})|j\rangle\langle j|D_m(\mathbf{r})\rangle$ and $\mathbf{\Phi}_{nm} = (\hbar^2/2m)\times\langle D_n(\mathbf{r})|\nabla B(\mathbf{r})\rangle\langle B(\mathbf{r})|\nabla D_m(\mathbf{r})\rangle$ are effective scalar potential matrices, with $|B(\mathbf{r})\rangle$ the bright state, i.e., the linear combination of ground states which couples with the excited state. Above, U_j is the energy of the state j, which includes the laser detunings from the corresponding transitions. Note also that U_j may be controlled by means of homogeneous magnetic fields and/or microwave dressing (as in recent experiments [6]).

The exact form of $\mathbf{A}_{nm}$, $\mathbf{\Phi}_{nm}$, and $\mathbf{V}_{nm}$ depends on the laser beams and their relative phase and intensity ratios. To obtain nontrivial gauge potentials the light fields need to be shaped carefully. There are many techniques to shape light fields in 2D [35]. Shaping arbitrary light beams in 3D is more challenging but certainly possible [36,37]. This results in a remarkable flexibility to achieve different gauge fields [5]. In this Letter we are particularly interested in externally inducing an effective SO coupling. This may be achieved by employing three copropagating lasers along, e.g., the z axis ($S_1 = S_2 = S_3 = kz$), with constant $|\Omega_3|$ and spatially dependent transversal profiles $\Omega_1 = |\Omega_3|\cos\phi(x,y)$, $\Omega_2 = |\Omega_3|\sin\phi(x,y)$. Assuming an intensity modulation along x such that $\phi(\mathbf{r}) = -\sqrt{2}\kappa x$, we obtain the effective SO coupling $\mathbf{A} = -\hbar\kappa\hat{\sigma}_y\vec{e}_x$ [5], which we employ in our discussion of the 1D localized solutions. If the intensity modulation has a polar symmetry on the xy plane, i.e., $\phi(\mathbf{r}) = -\sqrt{2}\kappa\rho$ (with $\rho^2 = x^2 + y^2$), then $\mathbf{A} = -\hbar\kappa\hat{\sigma}_y\vec{e}_\rho$, which we consider for the case of 2D chiral confinement. Finally, setting $U_{-1} = U_0 = \hbar\Delta - \hbar^2\kappa^2/2m$, and $U_1 = -U_{-1} - 2\hbar\Delta$, one obtains for both 1D and 2D arrangements $\mathbf{\Phi} + \mathbf{V} = \hbar\Delta\hat{\sigma}_z$. We will in the following assume $\Delta < 0$.

The term $\mathbf{p}\cdot\boldsymbol{\sigma}$, where $\boldsymbol{\sigma} = \hat{\sigma}_y\vec{e}_{x,\rho}$ leads to a single-atom dispersion law characterized by two branches $E_\pm(p) = (p^2 + \hbar^2\kappa^2)/2m \pm (\hbar^2\Delta^2 + \hbar^2\kappa^2p^2/m^2)^{1/2}$. The E_- branch presents two minima (or a continuous ring of minima). As a result the ground state of the many-body system may become fragmented [38]. Fragmentation would preclude the use of the Gross-Pitaevskii (GP) formalism employed below. The analysis is, however, well justified if we consider an initial (well-defined) scalar BEC in one of the ground-state levels, and adiabatically switch on the lasers, which allows a transfer of the BEC (in the absence of dissipation) into the dark-state manifold [6,39].

Interatomic interactions are crucial in quantum gases. We assume the interaction energy is much smaller than $\hbar\Omega$, such that we remain in the dark-state manifold. Note that the states $|-1, 0, 1\rangle$ constitute a spin-1 Bose gas. Short-range interactions are dominantly s wave and occur only in channels with total spin 0 and 2, characterized by the scattering lengths $a_{0,2}$ [26]. Although a_0 and a_2 are in principle different, in practice they are very similar. Below we consider for simplicity $a_0 = a_2 = a$ and repulsive interactions, $a > 0$. For $a_0 \neq a_2$ the system remains in the dark-state manifold, but the equations are much more complicated and may present collisionally induced spin rotations. The interactions in d dimensions are characterized by a coupling constant $g = 4\pi\hbar^2aN/m(\sqrt{2\pi}l_\perp)^{3-d}$, where N is the particle number, and $l_\perp$ is the oscillator length associated to a harmonic transversal confinement.

Within the GP formalism, the interacting bosons in the dark-state manifold are described by a spinor GP-like equation with a SO coupling, which in its time-independent form becomes

$$\mu\vec{\Psi} = \left[\frac{1}{2m}(\mathbf{p} + \hbar\kappa\boldsymbol{\sigma})^2 + \hbar\Delta\hat{\sigma}_z + g\vec{\Psi}^\dagger\cdot\vec{\Psi}\right]\vec{\Psi}, \qquad (2)$$

where μ is the chemical potential. Note that the interaction term $g\vec{\Psi}^\dagger\cdot\vec{\Psi} = g|\Psi_1|^2 + g|\Psi_2|^2$ is particularly simple since $a_0 = a_2$. For a wave packet with $\langle p\rangle = 0$ and momentum width $\delta p \ll 2\hbar\kappa, \sqrt{2\hbar|\Delta|m}$ we can safely neglect the $\mathbf{p}^2$ term in Eq. (2). This results in a NLDE:

$$\varepsilon\vec{\Psi} = [i\boldsymbol{\sigma}\cdot\nabla + \hat{\sigma}_z - \gamma\vec{\Psi}^\dagger\cdot\vec{\Psi}]\vec{\Psi}, \qquad (3)$$

where $\varepsilon = \mu/\hbar\Delta$, $\gamma = g/\hbar|\Delta|l_0^d$, and the unit of length is $l_0 = \hbar\kappa/m|\Delta|$. As discussed below, the solutions which follow have a typical width $\gtrsim l_0$. As a consequence, neglecting the p^2 term is valid only for $|\Delta| \ll 2\hbar\kappa^2/m$. Note that ε can here be negative, which allows for an interesting symmetry in the problem. Equation (3) can also be obtained if $\Delta > 0$, $g < 0$, and $\mathbf{A} \to -\mathbf{A}$ [which may be achieved by choosing $-\phi(\mathbf{r})$ instead of $\phi(\mathbf{r})$]. Hence, by properly choosing the sign of Δ and $\mathbf{A}$, which are easily controlled externally, one can get similar solutions for both repulsive and attractive interatomic interactions.

Interestingly, it has been shown in the context of chiral confinement in the massive Thirring and Gross-Neveu models that Eq. (3) supports in the 1D case an exact self-localized solution [27,28]. In the following we show that these 1D self-trapped solutions present remarkable properties, which have not been explored in the high-energy context due to the limitations of the original physical models. In addition, we show that multidimensional confinement is also possible, although it differs significantly from the 1D case.

We study first a 1D scenario (along x), assuming a strong yz harmonic trap with frequency $\omega_\perp$, such that $\hbar\omega_\perp \gg |\mu|$. We consider a SO coupling $\mathbf{p}\cdot\boldsymbol{\sigma} = p_x\hat{\sigma}_y$. Using $\vec{\Psi} = \eta(\cos\varphi, \sin\varphi)^T$, Eq. (3) transforms into

$$\frac{d\varphi}{dx} = \varepsilon - \cos(2\varphi) + \gamma\eta^2, \tag{4}$$

$$\frac{d\eta}{dx} = -\eta\sin(2\varphi). \tag{5}$$

which lead to $\eta^2(\varepsilon^2 + \gamma\eta^2/2 - \cos 2\varphi) = \text{const}$. Imposing localization ($\eta \to 0$ for $x \to \pm\infty$) one obtains $\varepsilon + \gamma\eta^2/2 - \cos 2\varphi = 0$. Inserting this conservation law back in (4) and (5) we obtain the localized solution [27]

$$\varphi(x) = \tan^{-1}[\sqrt{\beta}\tanh(\lambda x)], \tag{6}$$

$$\eta^2(x) = \frac{2(1-\varepsilon)/\gamma}{\cosh^2(\lambda x) + \beta\sinh^2(\lambda x)}, \tag{7}$$

where we have introduced the notation $\beta = (1-\varepsilon)/(1+\varepsilon)$ and $\lambda = \sqrt{1-\varepsilon^2}$. From these expressions it is clear that only solutions with $|\varepsilon| < 1$ (i.e., $|\mu| < \hbar|\Delta|$) are localized.

Imposing the normalization of the 1D wave function $\int_{-\infty}^{\infty} dx\eta^2 = 1$ leads to the condition $\gamma = 4\tan^{-1}\sqrt{\beta}$. Hence, both normalization and localization conditions are fulfilled only for $0 < \gamma < 2\pi$ [40]. In this regime the energy presents a remarkable sinusoidal dependence $\varepsilon = \cos(\gamma/2)$. Note that contrary to the high-energy case, where the constraint to positive energy fermion states demands $\gamma \leq \pi$ [27], in ultracold gases $\gamma > \pi$ is also possible. This leads to a peculiar behavior of the BEC wave function when γ approaches 2π. For $0 < \gamma < 2\pi$ the half width at half maximum of the soliton is $\text{arccosh}[\sqrt{(3+\varepsilon)/2}]/\sqrt{1-\varepsilon^2}$ which diverges at $\varepsilon = 1$, i.e., $\gamma = 0$, due to the absence of interactions. On the contrary, for $\varepsilon = 1$ or $\gamma = 2\pi$, the localized solution does exist but acquires a Lorentzian form $1/(1+4x^2)$.

These localized wave functions are solutions of the linear in p Eq. (3). However the quadratic term p^2 induces a departure from these solutions, which becomes significant at a time scale $\tau \sim 2m/\hbar\kappa^2$. We have quantitatively analyzed the effects of p^2 by numerically solving Eq. (2) for different values of $2m|\Delta|/\hbar\kappa^2$ and of γ, using as the initial condition the above mentioned localized solutions. Figure 1 shows typical results. As expected, the linear solutions are only significantly modified for times $t \gtrsim \tau$. The p^2 term does not actually lead to a destruction of the soliton but to a modulation of its width and height.

Because of the form of $\varphi(x)$, the relative distribution of the population between the two components also presents a peculiar dependence in γ. The population imbalance χ between $|D_1\rangle$ and $|D_2\rangle$ becomes $\chi = \int dx\eta^2\cos(2\varphi) = \frac{2}{\gamma}\sin(\gamma/2)$, which monotonically decreases from 1 (all atoms in $|D_1\rangle$) at $\gamma = 0$ to 0 (equal admixture of both dark states) at $\gamma = 2\pi$. The density profile of both components is also quite different, since $|D_2\rangle$ presents a node at $x = 0$, whereas $|D_1\rangle$ is maximal at the center.

Note that the discussed sinusoidal dependence has its origin in the 1D normalization of η^2. We should hence expect a rather different behavior in higher dimensions. This is indeed the case. We consider in the following a 2D scenario on the xy plane with a strong confinement along z,

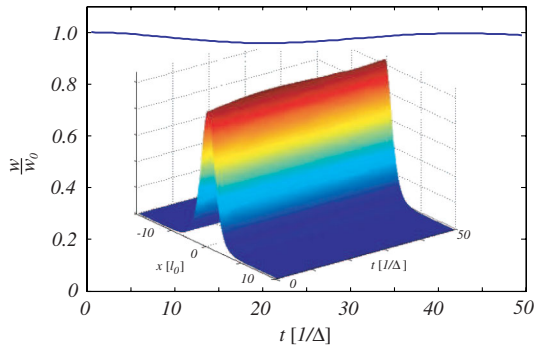

FIG. 1 (color online). Normalized width $w/w_0 = \sqrt{\int dx x^2\eta(t)^2 / \int dx x^2\eta(0)^2}$ of the localized 1D solutions for $2m\Delta/\hbar\kappa^2 = 0.01$ and $\gamma = \pi/3$. In the inset, we depict the time evolution of the total BEC density.

in the presence of a SO coupling $\mathbf{p}\cdot\boldsymbol{\sigma} = p\hat{\sigma}_y$, where $p^2 = p_x^2 + p_y^2$. Equations (6) and (7) can be readily generalized to the 2D case by replacing x by the radial coordinate ρ. The normalization of (7) is, however, different, $2\pi\int\rho\eta^2(\rho)d\rho = 1$, which requires $\gamma = 4\pi[s\ln 2 - L(s)]/\sin(2s)$, where $\varepsilon = \cos(2s)$ $(0 \leq s \leq \pi/2)$ and $L(s) = -\int_0^s \ln(\cos s')ds'$ is the Lobachevsky function [41]. By inverting the expression for γ we obtain $\varepsilon(\gamma)$ (Fig. 2). As mentioned above a localized solution requires $|\varepsilon| \leq 1$, which is only possible for $\gamma > \gamma_c = 2\pi\ln 2 \simeq 4.36$ [42]. Therefore, contrary to the 1D localization which may occur for $0 < \gamma < 2\pi$, the 2D localized BEC requires a minimal interaction strength γ_c at which the BEC width diverges. In addition, both localization and normalization conditions are simultaneously fulfilled for arbitrary $\gamma > \gamma_c$. For increasing $\gamma > \gamma_c$, ε decreases monotonically from 1 to -1. For $\gamma \gtrsim 15$, $\varepsilon \simeq -1$ and the localized wave function converges to a Lorentzian shape $\eta^2(\rho) = 8\pi\gamma^{-1}(1+4\rho^2)^{-1}$. Figure 3 shows 2D localized BECs. Note that the behavior of the population imbalance χ in 2D differs from the 1D case. In particular for $\varepsilon \to 1$, $\chi \to 1$ as in 1D, and for $\varepsilon \to -1$, $\chi \to -1$; i.e., $|D_2\rangle$ dominates. Note also that as in 1D the $|D_2\rangle$ state has a minimum at the center, whereas $|D_1\rangle$ is there maximal. This broken symmetry between $|D_1\rangle$ and $|D_2\rangle$ is induced by the $\Delta\sigma_z$ term in the equation of motion.

Finally, a similar solution may occur also in 3D if $\mathbf{p}\cdot\boldsymbol{\sigma} = p\hat{\sigma}_y$, where $p^2 = p_x^2 + p_y^2 + p_z^2$. In this case the 3D

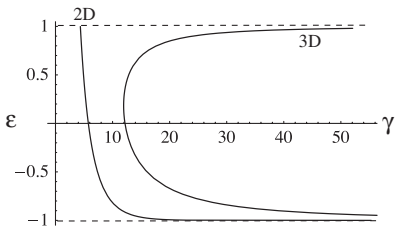

FIG. 2. Energy ε as a function of the interaction strength γ for a 2D and 3D arrangement. Note the existence of a 2D solution for $\gamma > 4.36$ and a double 3D solution for $\gamma > 11.94$.

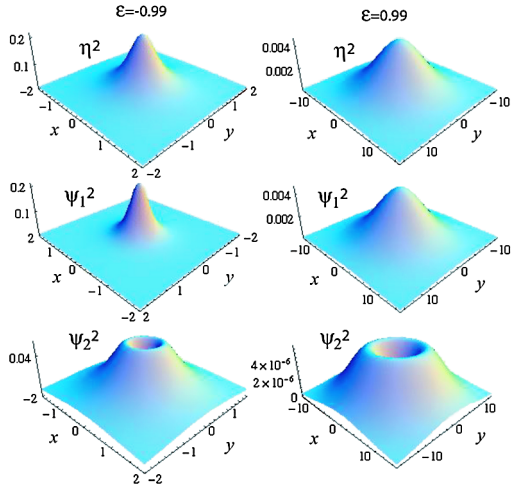

FIG. 3 (color online). Left column: 2D solution for $\varepsilon = -0.99$ and $\gamma = 18.63$. The total density η^2 is shown at the top. The density of each component $\Psi_{1,2}^2$ is strikingly different, with component 1 forming a peak in the center. Most particles occupy component 2. Right column: $\varepsilon = 0.99$ and $\gamma = 4.36$. Component 1 forms a peak in the center where now most particles are located. The x, y coordinates are in units of l_0 and the densities in units of $1/l_0^2$ (see text).

normalization requires that $\gamma = 2s(\pi^2 - 4s^2)/3\sin^2(2s)$ (Fig. 2). The localized solution exists only for $\gamma > \gamma_c \simeq 11.94$ [43]. Contrary to 2D where the BEC width diverges at γ_c and hence the wave function experiences a smooth crossover from localization into delocalization, in 3D at $\gamma = \gamma_c$, $\varepsilon < 1$ and the BEC width remains finite. Hence in 3D there is an abrupt transition between localization and delocalization regimes. Finally, let us point out that, interestingly, for $\gamma > \gamma_c$, there are actually two localized solutions. At $\gamma \to \infty$, one of the solutions becomes unbound and the other a Lorentzian shaped function.

In summary, the interplay between interactions and an optically induced SO coupling may lead to self-localized BECs in 1D, but also in 2D and 3D. Self-localization in NLDE was previously studied in the context of chiral confinement in massive Thirring and Gross-Neveu models. However, for the case of cold gases novel parameter regimes (and dimensionalities) are possible, allowing for remarkably rich physics which depends strongly on the system dimensionality, ranging from a sinusoidal interaction dependence in 1D, to two possible self-trapped solutions in 3D scenarios. These results provide exciting new perspectives for the nonlinear physics of condensates in artificially-induced gauge fields.

This work was supported by EPSRC U.K., DFG (SFB407, QUEST), and ESF (EUROQUASAR).

[1] See, e.g., F. Dalfovo *et al.*, Rev. Mod. Phys. **71**, 463 (1999).
[2] J. Ruostekoski, G. V. Dunne, and J. Javanainen, Phys. Rev. Lett. **88**, 180401 (2002).
[3] D. Jaksch and P. Zoller, New J. Phys. **5**, 56 (2003).
[4] K. Osterloh *et al.*, Phys. Rev. Lett. **95**, 010403 (2005).
[5] J. Ruseckas *et al.*, Phys. Rev. Lett. **95**, 010404 (2005).
[6] Y.-J. Lin *et al.*, Phys. Rev. Lett. **102**, 130401 (2009).
[7] Y.-J. Lin *et al.*, Nature (London) **462**, 628 (2009).
[8] J. Y. Vaishnav and C. W. Clark, Phys. Rev. Lett. **100**, 153002 (2008).
[9] V. Pietilä and M. Möttönen, Phys. Rev. Lett. **102**, 080403 (2009).
[10] G. Juzeliūnas *et al.*, Phys. Rev. A **77**, 011802(R) (2008).
[11] A. Jacob *et al.*, Appl. Phys. B **89**, 439 (2007).
[12] K. S. Novoselov *et al.*, Nature (London) **438**, 197 (2005).
[13] A. K. Geim and K. S. Novoselov, Nature Mater. **6**, 183 (2007).
[14] V. V. Cheianov, V. Fal'ko, and B. L. Altshuler, Science **315**, 1252 (2007).
[15] L. H. Haddad and L. D. Carr, Physica (Amsterdam) **238D**, 1413 (2009).
[16] J. Denschlag *et al.*, Science **287**, 97 (2000).
[17] S. Burger *et al.*, Phys. Rev. Lett. **83**, 5198 (1999).
[18] L. Khaykovich *et al.*, Science **296**, 1290 (2002).
[19] K. E. Strecker *et al.*, Nature (London) **417**, 150 (2002).
[20] B. Eiermann *et al.*, Phys. Rev. Lett. **92**, 230401 (2004).
[21] D. Ivanenko, Sov. Phys. **13**, 141 (1938).
[22] H. Weyl, Phys. Rev. **77**, 699 (1950).
[23] W. Heisenberg, Physica (Amsterdam) **19**, 897 (1953).
[24] M. Soler, Phys. Rev. D **1**, 2766 (1970).
[25] A. F. Rañada and M. F. Rañada, Phys. Rev. D **29**, 985 (1984).
[26] T.-L. Ho, Phys. Rev. Lett. **81**, 742 (1998).
[27] S. J. Chang, S. D. Ellis, and B. W. Lee, Phys. Rev. D **11**, 3572 (1975).
[28] S. Y. Lee, T. K. Kuo, and A. Gavrielides, Phys. Rev. D **12**, 2249 (1975).
[29] See, e.g., Yu. S. Kivshar and G. P. Agrawal, *Optical Solitons: From Fibers to Photonic Crystals* (Academic, San Diego, 2003).
[30] Th. Busch and J. R. Anglin, Phys. Rev. Lett. **87**, 010401 (2001).
[31] A. E. Muryshev *et al.*, Phys. Rev. A **60**, R2665 (1999).
[32] M. V. Berry, Proc. R. Soc. A **392**, 45 (1984).
[33] F. Wilczek and A. Zee, Phys. Rev. Lett. **52**, 2111 (1984).
[34] C. A. Mead, Rev. Mod. Phys. **64**, 51 (1992).
[35] R. W. Gerchberg and W. O. Saxton, Optik **35**, 237 (1972).
[36] Z. Bouchal and J. Kyvalsky, J. Mod. Opt. **51**, 157 (2004).
[37] G. Whyte and J. Courtial, New J. Phys. **7**, 117 (2005).
[38] T. D. Stanescu, B. Anderson, and V. Galitski, Phys. Rev. A **78**, 023616 (2008).
[39] K. J. Günter *et al.*, Phys. Rev. A **79**, 011604(R) (2009).
[40] $0 < N < 700$ for ^{87}Rb, $\kappa = 0.5$ μm and $\omega_\perp/2\pi = 1$ kHz.
[41] I. S. Gradshteyn and I. M. Ryzhik, *Table of Integrals, Series, and Products* (Academic Press, London, 1994).
[42] $N > 850$ for ^{87}Rb, $\kappa = 0.5$ μm, $\omega_\perp/2\pi = 1$ kHz, and $\Delta/2\pi = 1$ kHz.
[43] $N > 4000$ for ^{87}Rb, $\kappa = 0.5$ μm, and $\Delta/2\pi = 1$ kHz.